



This is a repository copy of *Development of new metrics to assess and quantify climatic drivers of extreme event driven Arctic browning*.

White Rose Research Online URL for this paper:
<http://eprints.whiterose.ac.uk/160052/>

Version: Accepted Version

Article:

Treharne, R., Bjerke, J.W., Tømmervik, H. et al. (1 more author) (2020) Development of new metrics to assess and quantify climatic drivers of extreme event driven Arctic browning. *Remote Sensing of Environment*, 243. 111749. ISSN 0034-4257

<https://doi.org/10.1016/j.rse.2020.111749>

Article available under the terms of the CC-BY-NC-ND licence
(<https://creativecommons.org/licenses/by-nc-nd/4.0/>).

Reuse

This article is distributed under the terms of the Creative Commons Attribution-NonCommercial-NoDerivs (CC BY-NC-ND) licence. This licence only allows you to download this work and share it with others as long as you credit the authors, but you can't change the article in any way or use it commercially. More information and the full terms of the licence here: <https://creativecommons.org/licenses/>

Takedown

If you consider content in White Rose Research Online to be in breach of UK law, please notify us by emailing eprints@whiterose.ac.uk including the URL of the record and the reason for the withdrawal request.



eprints@whiterose.ac.uk
<https://eprints.whiterose.ac.uk/>

1 **Title: Development of new metrics to assess and quantify climatic drivers of extreme**
2 **event driven Arctic browning.**

3

4 **List of authors:**

Rachael Treharne¹, Jarle W. Bjerke², Hans Tømmervik², Gareth K. Phoenix¹.

¹Department of Animal and Plant Sciences, The University of Sheffield, Western Bank,
Sheffield, S10 2TN, UK

²Norwegian Institute for Nature Research, FRAM – High North Research Centre for Climate
and the Environment, NO-9296 Tromsø, Norway

5 **Corresponding author:**

6 Rachael Treharne¹

¹Department of Animal and Plant Sciences, The University of Sheffield, Western Bank,
Sheffield, S10 2TN, UK

7 rtreharne1@sheffield.ac.uk

8 +44(0)7788765609

9

10 **Keywords:** Arctic, climate change, extreme events, climate metrics, browning, winter,
11 NDVI, heathland, sub-Arctic, ericoid shrubs

12 **Type of Paper:** Primary research article

13 **Abstract**

14 Rapid climate change in Arctic regions is resulting in more frequent extreme climatic events.
15 These can cause large-scale vegetation damage, and are therefore among key drivers of
16 declines in biomass and productivity (or “browning”) observed across Arctic regions in recent
17 years.

18 Extreme events which cause browning are driven by multiple interacting climatic variables,
19 and are defined by their ecological impact – most commonly plant mortality. Quantifying the
20 climatic causes of these multivariate, ecologically defined events is challenging, and so existing
21 work has typically determined the climatic causes of browning events on a case-by-case basis
22 in a descriptive, unsystematic manner. While this has allowed development of important
23 qualitative understanding of the mechanisms underlying extreme event driven browning, it
24 cannot definitively link browning to specific climatic variables, or predict how changes in these
25 variables will influence browning severity. It is therefore not yet possible to determine how
26 extreme events will influence ecosystem responses to climate change across Arctic regions.

27 To address this, novel, process-based climate metrics that can be used to quantify the conditions
28 and interactions that drive the ecological responses defining common extreme events were
29 developed using publically available snow depth and air temperature data (two of the main
30 climate variables implicated in browning). These process-based metrics explained up to 63%
31 of variation in plot-level Normalised Difference Vegetation Index (NDVI) at sites within areas
32 affected by extreme events across boreal and sub-Arctic Norway. This demonstrates potential
33 to use simple metrics to assess the contribution of extreme events to changes in Arctic biomass
34 and productivity at regional scales. In addition, scaling up these metrics across the Norwegian
35 Arctic region resulted in significant correlations with remotely-sensed NDVI, and provided
36 much-needed insights into how climatic variables interact to determine the severity of
37 browning across Arctic regions.

39 **1 Introduction**

40 An increase in frequency of climatic extreme events is among the most marked consequences
41 of climate change (IPCC, 2017). In the Arctic, climate change is progressing faster than almost
42 anywhere else in the world, especially during winter (AMAP, 2017), and increases in extreme
43 events - particularly those associated with winter climate - are therefore being observed
44 (Vikhamar-Schuler et al., 2016, Graham et al., 2017). Although traditionally, climate change
45 research has focussed on changes in mean conditions, it is now recognised that extreme events
46 can have major impacts on ecosystems (Zscheischler et al., 2014, Solow, 2017). In Arctic
47 regions, these impacts include considerable changes in vegetation biomass, productivity and
48 phenology (Bokhorst et al., 2008, Jepsen et al., 2013, Reichstein et al., 2013). However, proper
49 quantitative understanding of the climatic drivers that cause these extreme event impacts is
50 currently lacking, since research has so far focussed on an 'impact orientated' approach, where
51 ecological consequences are studied in detail, while climatic drivers are generally defined in
52 qualitative, descriptive terms.

53

54 This is of concern since extreme events linked to winter climate change are already causing
55 major disturbance in the form of sudden mortality and extreme stress in widespread Arctic and
56 sub-Arctic vegetation, with the potential to cause large scale and magnitude impacts, such as
57 the record low productivity of the Nordic Arctic Region (NAR) observed in 2012 (Bokhorst et
58 al., 2009, Bjerke et al., 2014, 2017). Such events include, for example, transient periods of
59 extreme winter warmth, leading to premature dehardening and frost damage (extreme winter
60 warming), or exposure to cold, wind and irradiance following loss of snow cover, leading to
61 severe desiccation damage (frost drought). These are important drivers of 'Arctic browning', a
62 decline in biomass and productivity observed across Arctic regions in recent years (Epstein *et*

63 *al.*, 2015, 2016, Phoenix & Bjerke, 2016). However, although remotely sensed Normalised
64 Difference Vegetation Index (NDVI) has been used to assess the extent and impacts of extreme
65 events identified during field studies (Bokhorst et al., 2009), detecting events using this
66 approach is challenging (Treharne et al., 2018). Methods to quantitatively define climatic
67 drivers of extreme event driven browning are therefore needed before the contribution of
68 extreme events to remotely-sensed vegetation change across Arctic regions can be fully
69 determined.

70

71 Extreme events are typically defined using climatological thresholds or using an impact-
72 orientated definition (van de Pol et al., 2017). The latter approach may define an extreme event
73 as one where the ability of an organism to acclimate is substantially exceeded (Gutschick &
74 BassiriRad, 2003) or as a climatologically rare event that alters ecosystem structure or function
75 outside the bounds of normal variability (Smith et al., 2011). Impact orientated definitions are
76 commonly used for ‘compound events’; events driven by combinations of interacting variables
77 which separately may not trigger an extreme response, but, together, cross ecological
78 thresholds to trigger an extreme response (van de Pol et al., 2017). Extreme climatic events
79 which drive Arctic browning, such as frost drought and extreme winter warming, are examples
80 of compound events. These events have therefore so far been defined by their biological
81 impacts; most clearly vegetation mortality (Bokhorst et al., 2011) or a marked visible stress
82 response indicated by persistent anthocyanin pigmentation (Bjerke et al., 2017).

83

84 Events such as these which are defined by an ecological impact and driven by a combination
85 of multiple climatic variables are especially complex to quantify, compare or predict
86 (Easterling et al., 2000). This complexity is compounded when the physiological thresholds
87 beyond which an extreme response is triggered are likely to differ with event timing, preceding

88 conditions and the occurrence of successive events (Knapp et al., 2015, Sippel et al, 2016, Wolf
89 et al, 2016, Ummenhofer & Meehl 2017). This is particularly relevant in Arctic regions, where
90 the depth and extent of insulating snow cover determines whether vegetation is exposed to
91 ambient conditions such as air temperature (Williams et al., 2014; Bokhorst et al., 2016), where
92 event timing may drastically change the conditions to which vegetation is exposed, such as
93 light intensity, and where susceptibility to an extreme response may be heavily dependent on
94 preconditioning, such as the duration of chilling prior to an extreme winter warming event,
95 which could determine susceptibility to premature loss of winter freeze tolerance
96 (dehardening).

97

98 In common with much extreme event literature (Bailey & van de Pol, 2015, Altwegg et al.,
99 2017), assessment of the multivariate climatic drivers in studies of extreme event driven Arctic
100 browning is therefore typically descriptive and unsystematic, dealing with a single event or a
101 few, often differing, events. Nonetheless, these studies have provided critical insights into these
102 events, including a qualitative understanding of event drivers and quantification of major
103 impacts on vegetation growth, phenology and productivity, and on ecosystem CO₂ fluxes
104 (Bokhorst et al., 2008, 2009, 2011; Bjerke et al., 2014, 2017; Parmentier et al., 2018). However,
105 their ability to attribute these measured responses definitively to specific hypothesised climatic
106 drivers is limited. In addition, this approach cannot determine where response thresholds lie,
107 or therefore predict how the severity of the browning response could scale with different
108 climate variables, or when specific conditions might be expected to result in vegetation
109 damage.

110

111 This is of concern given the scale of observed browning impacts, which include substantial
112 loss of biomass at landscape or greater scales (Bjerke et al., 2014, 2017) and large changes in

113 ecosystem CO₂ fluxes with significant implications for landscape-level carbon balance.
114 Furthermore, as the frequency of many types of extreme climatic event is predicted to increase
115 in Arctic regions as climate change progresses, the scale and extent of these impacts are likely
116 to increase (Vikhamar-Schuler et al., 2016, Graham et al., 2017). To fully understand how these
117 events will influence the responses of Arctic ecosystems to climate change, a more systematic
118 approach is needed; correlating measured response to specific, process-based climatic
119 variables. As a first step, a framework to quantify the drivers of extreme event-driven Arctic
120 browning, and the interactions between them, is required to understand how variation in these
121 drivers influences the severity of response in vegetation communities, and ultimately drives
122 browning. This quantitative understanding is critical to identify the contribution of extreme
123 events to Arctic browning trends at regional scales, and to fully understand how winter climate
124 change will impact Arctic plant communities.

125

126 Therefore, the aims of this work were to apply established ecological understanding about the
127 drivers of specific instances of extreme event driven browning to (a) identify simple, process-
128 based, quantitative climate metrics that can be used to quantify extreme winter conditions in a
129 systematic, comparable way and (b) assess the relationship between these metrics and changes
130 in satellite NDVI at regional scales. The development of climate metrics initially utilised a
131 dataset of plot-level measurements of NDVI and visible vegetation damage across 19 sites
132 known to have been affected by extreme winter climatic events (primarily frost drought and
133 extreme winter warming experienced during the 2013/14 winter) and subsequent browning.
134 Following this, national meteorological and modelled snow cover datasets were used to
135 compare climate metrics with remotely sensed NDVI across the Norwegian Arctic region. It
136 was hypothesised that (a) simple climate metrics will be identified that correlate with NDVI in
137 areas known to have been affected by browning, (b) these metrics will reflect ecological

- 138 understanding about the mechanisms underlying extreme climatic event driven browning, and
- 139 (c) these metrics will correlate with NDVI change at regional scales.

140 **2 Methods**

141 **2.1 Developing climate metrics using plot-scale analysis**

142 *2.1.1 Plot-level NDVI*

143

144 Widespread browning of evergreen shrubs across boreal and sub-Arctic regions of Norway was
145 observed following the 2013/14 winter, attributed to extreme winter weather conditions
146 (Meisingset et al., 2015; Bjerke et al. 2017). For this plot-scale analysis, observations of
147 browning recorded in the growing seasons following these extreme winter conditions (2014 or
148 2015) were collated from 19 sites (Fig. 1) in boreal and sub-Arctic Norway. The number of
149 plots at each site ranged from 1 to 143 (with a mean of 19), with each plot measuring 1 x 1m.
150 Replicate plots were located at least 2 m apart and were chosen to reflect the full range of
151 observed browning, including green, healthy vegetation apparently unaffected by extreme
152 events (control plots). Browning at the majority of these sites was driven by the extreme
153 conditions during the 2013/14 winter, with remaining sites browned during previous winters
154 (2011/12 at the earliest; Bjerke et al., 2014). Observations consisted of plot-level NDVI
155 measurements and/or visual assessments of plant damage (mortality; observed as browning).
156 NDVI measurements were taken using either digital NDVI cameras (passive NDVI sensors),
157 in which the usual light sensor is replaced with an infrared sensor, enabling the camera to record
158 visible light in the blue channel and near infrared in the red channel (Llewellyn Data
159 Processing, New Jersey), or an active NDVI sensor (Greenseeker; Trimble, California). The
160 Greenseeker NDVI sensor emits red and infrared light and measures the reflectance of each
161 wavelength in terms of the normalized difference vegetation index (NDVI) and is mainly used
162 in precision agriculture (Bourgeon et al., 2017) and in phenological monitoring; including of
163 browning trends and events in the Arctic (Anderson et al. 2016; Bokhorst et al., 2018). The
164 visual assessments of browning were recorded either as percentage cover of browned
165 vegetation (mortality), or the proportion of the dominant species affected by browning (own
166 data and data provided by J. Bjerke). NDVI and observed browning (plot survey) were

167 significantly correlated. This correlation was calculated separately across plots within each of
168 the three Norwegian counties of Troms, Nordland and Nord-Trøndelag to allow for some
169 regional variation while minimising the loss of statistical power ($p < 0.05$ in all cases). The
170 correlation was then used to predict plot-level NDVI at plots where observed browning alone,
171 and not NDVI, was recorded.

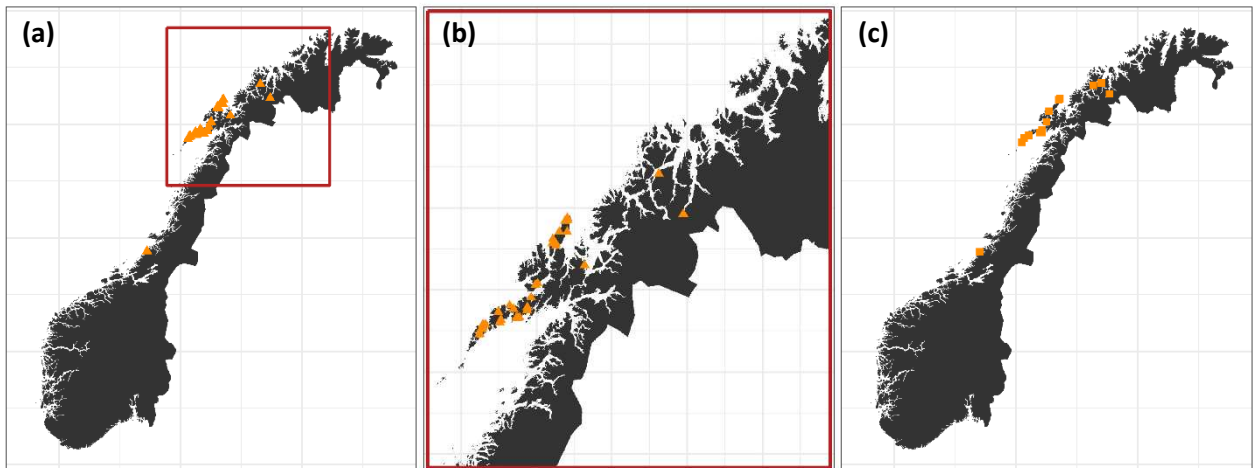


Figure 1: (a) Map of Norway showing locations of 19 sites (orange triangles) where extreme event-driven browning was observed and plot-level NDVI was measured. The Norwegian Arctic Region, the area used for regional level analysis, is outlined in red. This area is shown separately and enlarged in (b). The locations of the weather stations from which climatic data was analysed are shown in (c).

172

173 In addition, a ‘pre-browning’ NDVI value was estimated for each site. This ‘pre-browning’
174 value was assigned to the growing season preceding the winter during which browning
175 occurred (i.e. 2013 for the majority of sites). To estimate these pre-browning values, linear
176 regressions of NDVI and observed browning were calculated separately for each county ($p <$
177 0.05) and used to predict NDVI in vegetation with no observed browning. This approach
178 produced ecologically sensible estimates for healthy dwarf-shrub heathland NDVI of between
179 0.67 and 0.75 (Street et al., 2007). At two sites, 5-6 NDVI values in undamaged vegetation
180 adjacent to observed browning plots were recorded; in these cases recorded NDVI values in
181 undamaged vegetation were averaged to estimate pre-browning values for those sites.

182

183 *2.1.2 Climate data*

184 Snow depth maps of Norway with a daily temporal and 1 x 1 km spatial resolution were
185 obtained from The Norwegian Water Resources and Energy Directorate (NVE). This publically
186 available data is produced using the SeNorge snow model (<http://www.senorge.no>), which is
187 forced by daily observations of temperature and precipitation and performs well in Norway
188 (Saloranta, 2012).

189

190 From SeNorge snow maps, daily snow depth values were extracted from each pixel which
191 contained plot-level browning observations in the dataset described above. This data was
192 extracted for each winter between 2011 and 2015. Daily snow depth values for each site were
193 then obtained by taking a simple average across the pixels containing plot-level browning
194 observations for each site.

195

196 Daily mean, minimum and maximum air temperature was obtained from the Norwegian
197 Meteorological Institute via the publically available eklima.no web portal. Data for 2011 –
198 2015 was downloaded from the weather stations closest to each site (maximum distance <
199 25km) at an elevation of < 200m (as sites were located in relatively low-lying areas). Based on
200 the quality and availability of air temperature data from these stations, data from 14 stations
201 was subsequently analysed. See Fig. 1c for weather station locations.

202

203 *2.1.3 Development of metrics*

204 Snow and air temperature data was combined into a single dataset. Only data from the winter
205 period was used to develop climate metrics, to avoid any confounding effect of occasional late

206 spring or summer snowfall. To identify an appropriate window for this winter period during
207 which snow cover and cold temperatures could reasonably be expected, and therefore during
208 which warmth and exposure may have ecological consequences, first winter snow fall and final
209 spring snow melt for each winter (2011/12 – 2014/15) were identified. This was done by
210 selecting all periods of absent snow cover (0 mm snow depth) throughout the year; first winter
211 snowfall and final spring melt were recorded as the dates following and preceding the long
212 summer exposure period in consecutive years. Winter was thus defined from Day of Year 305
213 (Day of Winter 1) to Day of Year 120 (Day of Winter 181 or 182). A consistent winter period
214 was used rather than defining when winter began and finished each year separately (based on
215 climate data). This was because the latter approach might exclude periods of unseasonable
216 warmth or absent snow cover in early or late winter, since these periods would not be classed
217 as winter.

218

219 Within each winter a set of approaches were used to extract ‘events’ which may have
220 influenced NDVI. These were ‘exposure events’ based on absent snow cover (0 mm snow
221 depth) or ‘warming events’ based on warm winter temperatures ($> 2\text{ }^{\circ}\text{C}$). A $2\text{ }^{\circ}\text{C}$ threshold for
222 warming events was chosen based on assessment by eye of plotted temperature data during
223 warming events known to have resulted in browning, with this temperature found to ensure the
224 full duration of any warming event was captured. Furthermore, differentiation between short,
225 relatively mild warming events and prolonged periods of high temperatures was subsequently
226 facilitated by an ‘intensity’ metric (below and Table 1). Periods of exposure or warming
227 occurring before initial winter snowfall or cold temperatures were excluded. The variables
228 recorded for each event type were chosen based on the mechanism of damage particularly
229 associated with either winter warming (i.e. premature dehardening and initiation of spring-like
230 bud burst, followed by frost damage on the return of cold temperatures) or frost drought (loss

231 of snow cover and subsequent exposure, leading to gradual desiccation as transpiration exceeds
232 uptake from frozen or near-frozen soils) (Table 1). These two processes account for the
233 majority of reported extreme climatic event-driven browning in mainland Norway (e.g.
234 Hørbye, 1882; Printz, 1933; Bokhorst et al., 2009, 2012; Bjerke et al. 2014, 2017). Thus, for
235 exposure events (most likely to be associated with frost), event duration, start date and mean
236 air temperature were recorded. For warming events (most likely to be associated with extreme
237 winter warming), a wider range of variables were recorded (Table 1). These include the
238 intensity metric, calculated as air temperature*duration. Weighting air temperature in this way
239 reflects the process through which extreme winter warming drives browning; exposure to
240 temperatures of sufficient warmth and duration to (a) melt snow and expose vegetation, and
241 then (b) subsequently initiate bud burst and premature loss of freeze tolerance.

242

243 Using this approach, several events were extracted for each year. To select those most likely to
244 influence growing season NDVI, up to 4 events were selected for each year. These were (a)
245 ‘Maximum intensity warming events’; the warming event with the highest ‘Intensity’ (air
246 temperature*duration; Table 5.1), (b) ‘Temperature drop warming events’; the warming event
247 with the greatest 24-h temperature drop following the final day of the event, (c) ‘Maximum
248 duration exposure events’; the maximum duration exposure event (i.e. no snow cover) (d)
249 ‘Maximum warmth exposure events’; the warmest exposure (no snow cover) event.

Table 1: Variables (climate metrics) recorded for each event type (either warming events based on consecutive daily air temperatures of > 2°C, or exposure events based on consecutive days of absent (0mm) snow cover) as extracted from snow depth and air temperature data.

Variable	Meaning	Event type
Count	Event duration (days).	Warming; Exposure
Start date	Date (Day Of Winter) of the first day of the event.	Warming; Exposure
Intensity	Cumulative mean daily air temperature (°C) linearly weighted by duration throughout the event. E.G. for a 3 day event with daily mean air temperatures of 4°C, 6°C and 3°C, Value = (4*1) + (6*2) + (3*3) = 25.	Warming
Mean snow depth	Mean snow depth (mm) during the event.	Warming
Mean air temperature	Mean air temperature (°C) during the event.	Exposure
End minimum temperature	Minimum temperature 24 hours following the final day of the event (°C).	Warming
24 hour temperature drop	Difference between mean daily air temperature on the last day of the event and minimum air temperature 24 hours later (°C).	Warming
5 day temperature mean	Mean daily air temperature over the 5 days following the event (°C).	Warming

250

251

252 2.1.4 Satellite NDVI

253 Remotely sensed NDVI data were extracted from the publically available MOD13Q1 version

254 6 dataset. MOD13Q1 provides level 3 16-day composites of vegetation indices at 250 m

255 resolution in a sinusoidal projection. Tiles were downloaded for DOY 193 in 2015, the nearest

256 date to when plot-level measurements were recorded, using USGS Earth Explorer. These tiles

257 were re-projected to the UTM Zone 33 projection using the NASA HDF-EOS To GeoTIFF

258 Conversion Tool (HEG) and mosaicked to encompass the full extent of plot-level data. At the

259 plot-scale analysis stage, remotely sensed NDVI values were used only to test for an overall
260 correlation between plot-scale and remotely sensed NDVI values (supporting information).

261

262 *2.1.5 Statistical analysis*

263 Correlations between metrics representing selected events and subsequent growing season
264 NDVI were assessed by multiple regression. Selection of metrics with high explanatory power
265 for use in multiple regression was initially guided by tree-based regression analysis, following
266 which interactions included in multiple regression of each event type (a – d) against NDVI
267 were based on *a priori* knowledge and predictions relating to the mechanisms through which
268 each event may cause browning (Bokhorst et al., 2008; Bjerke et al., 2017). Terms and
269 interactions without a significant correlation with NDVI change were removed step wise. A
270 maximum of three terms was included in each multiple regression. Plot-level and MODIS
271 NDVI were compared by linear regression.

272

273 **2.2 Applying climate metrics at regional scales**

274 The Norwegian Arctic region (Fig. 2) was selected for upscaling as a clearly definable region
275 encompassing the majority of sites used for plot-level analysis. This area extends southwards
276 to the Arctic Circle (66° 33' N) and eastwards to the longitude of Magerøya, Finnmark (25°
277 40' E); the most northerly point of the Nordic Arctic Region (NAR, Bjerke et al., 2014).

278

279 *2.2.1 Satellite NDVI*

280 Both time integrated NDVI (TI-NDVI) and peak/maximum NDVI have been widely used in
281 Arctic vegetation studies (Stow et al., 2004). The TI-NDVI is considered as a robust proxy for
282 total growing-season productivity (Stow et al., 2004; Epstein et al., 2017). Remotely sensed
283 NDVI data were extracted from the publically available MOD13Q1 version 6 dataset described

284 above from the beginning of May (DOY 129) to the end of August (DOY 241). Tiles were
285 extracted for this period in 2014, as the most marked and widespread browning observed at
286 plot-level occurred during the 2013/2014 winter, and from 2005 to 2010 (inclusive) to create a
287 baseline period for comparison. Tiles were re-projected and mosaicked as described above.
288 Unvegetated areas ($NDVI < 0.12$) were masked out. Images were aggregated (by mean) to a 1
289 km resolution to facilitate comparison with climate data.

290 From this May-August NDVI dataset, time-integrated NDVI (TI-NDVI; the sum of NDVI
291 values during this period) was calculated for 2014 and the 2005-2010 baseline period. Change
292 detection was then carried out between 2014 and the 2005-2010 baseline period, producing TI-
293 NDVI change. This process was also carried out for mean July (approximately peak biomass)
294 NDVI.

295

296 2.2.2 *Climate data*

297 Data was obtained from The Norwegian Water Resources and Energy Directorate (NVE) and
298 the Norwegian Meteorological Institute as described above. To provide air temperature data
299 continuously across the Norwegian Arctic region, data was downloaded from every Norwegian
300 Meteorological Institute weather station with an elevation of $< 200\text{m}$ in the counties of
301 Nordland, Troms and Finnmark; a total of 77 stations. The 200m cut-off was used since above
302 this, weather stations tended to be on mountainsides, where data may be less representative of
303 the broader surrounding landscape and so be less suitable for interpolation (the majority of the
304 heathland vegetation typically affected by browning is in low lying regions). Mean daily air
305 temperature from each station was interpolated across these three counties using Inverse
306 Distance Weighted interpolation, before the resulting air temperature map was cropped to the
307 Norwegian Arctic region. Climate data (both air temperature maps and SeNorge snow maps)

308 were resampled using nearest neighbour assignment resampling to correspond to each other
309 and to MODIS data.

310

311 *2.2.3 Climate metrics*

312 Maximum intensity warming events and maximum duration exposure events were chosen to
313 investigate further in this analysis due to their high explanatory power in the plot-level analysis.
314 Extreme event metrics for these two event types were calculated as described above for the
315 2013/2014 winter within each 1 km pixel.

316

317 *2.2.4 Statistical analysis*

318 Multiple regressions of the parameters for each event type were carried out using Generalised
319 Least Squares against TI-NDVI change. This was also done for July NDVI change (change in
320 mid-season NDVI). All regressions were carried out at a 4 km resolution by aggregating raster
321 data to reduce computational intensity. As the Moran's *I* test indicated significant spatial
322 autocorrelation in model residuals, this was accounted for by using correlated error structures
323 (exponential, Gaussian, linear, spherical and rational quadratic) and selecting the appropriate
324 model error structure (rational quadratic for TI-NDVI and exponential for July NDVI)
325 according to the AIC criterion (Burnham & Anderson, 2002).

326 **3 Results**

327 **3.1 Climate metrics in plot-scale analyses**

328 Climatic events described by simple metrics were well correlated with plot-level NDVI.
329 ‘Maximum intensity warming events’ were calculated as the greatest value within a pixel of
330 sum of daily mean air temperature multiplied by event duration (i.e. intensity) in periods of
331 consistently warm ($> 2^{\circ}\text{C}$) winter air temperatures. The start day in winter, mean snow cover
332 and intensity of these events explained more than 60 % of variation in plot-level NDVI in
333 multiple regression (Fig. 2a; $F = 14.26$, D.F. = 4, 27, $p < 0.001$, $R^2 = 0.63$; see supporting
334 information for multiple regression formulae), with high intensity, later start day and lower
335 mean snow cover corresponding to lower NDVI values. ‘Temperature drop warming events’
336 were calculated as the periods of consistently warm air temperature ($> 2^{\circ}\text{C}$) with the greatest
337 drop in temperature during the 24 hours following the final day of the event. The start day and
338 intensity of these events explained almost 50% of variation in NDVI in multiple regression
339 (Fig. 2b; $F = 10.81$, D.F. = 3, 33, $p < 0.001$, $R^2 = 0.45$). Again, high intensity and later start
340 day were associated with lower NDVI. For both warming event types (maximum intensity
341 warming events and temperature drop warming events) there was a significant interaction
342 between intensity and start day ($p < 0.05$), meaning that the effect of intensity upon NDVI was
343 weaker later in the winter. Tree-based regression analysis (supporting information) of metrics
344 calculated for warming events also highlighted the 24-h temperature drop following an event
345 as a metric with high explanatory power for variation in NDVI; mean NDVI in plots which had
346 experienced a maximum intensity warming event with a 24-h temperature drop of more than
347 5.7°C was 0.2 (NDVI) lower than in those which had not. While the importance of the 24-h
348 temperature drop is of interest and provides some insight into mechanisms underlying plant
349 damage following warming events, its computational complexity (in particular its use of
350 minimum as well as mean air temperature datasets) meant that it was unsuitable for further
351 analysis within this work and was therefore not included in multiple regression analyses.

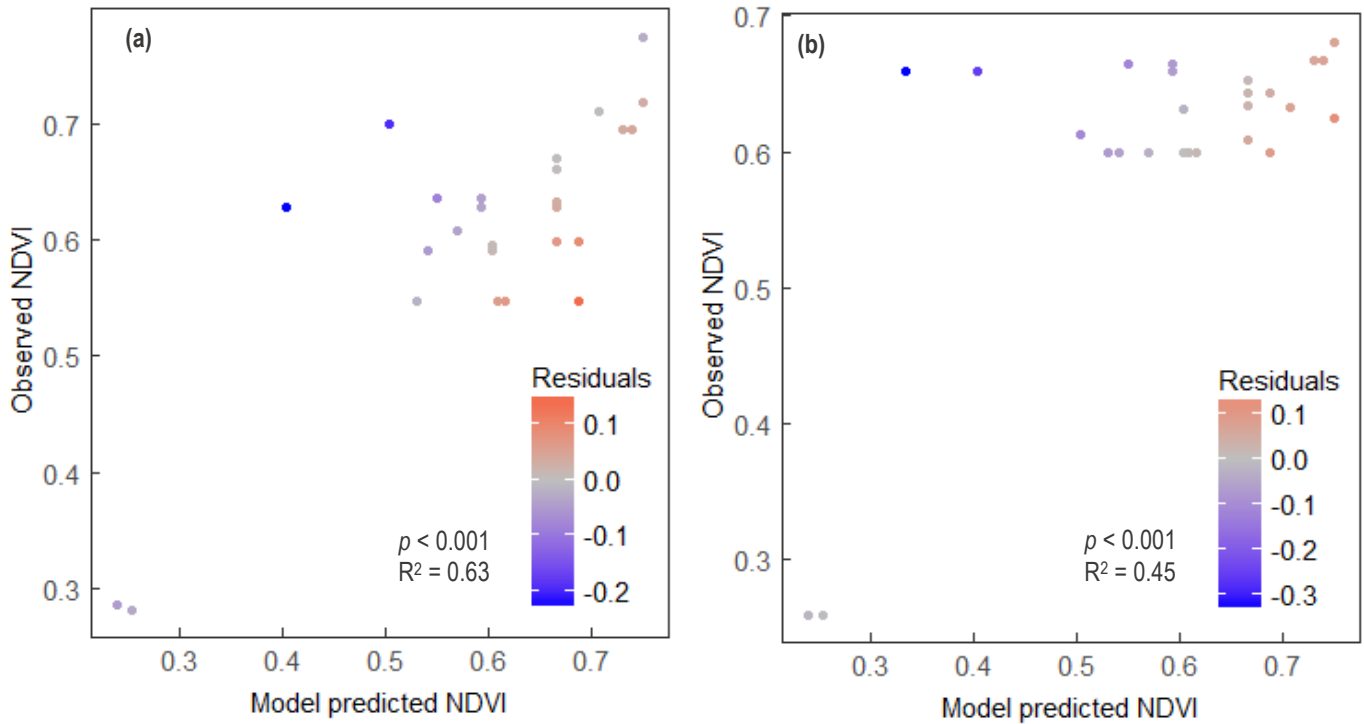


Figure 2: Correlations between plot-level NDVI as predicted by multiple regression models and plot-level NDVI observed in the field. Correlations are shown for (a) ‘Maximum intensity warming events’ and (b) ‘Temperature drop warming events’. Points are coloured according to the value of residuals; warm colouring indicates that multiple regression predicted higher NDVI values than were observed in the field, while cold colouring indicates that multiple regression predicted lower NDVI values than observed. See supporting information for explanation of number of visible data points.

352

353 ‘Maximum duration exposure events’ were calculated as the periods of consistently absent
 354 snow cover (0 mm snow depth) with the longest duration in days during winter. The start day
 355 of and mean temperature during these events were highly correlated with NDVI in multiple
 356 regression (Fig. 3a; $R^2 = 0.61$, $F = 17.87$, D.F. = 3, 29, $p < 0.001$). ‘Maximum warmth exposure
 357 events’ are the periods of consistently absent snow cover with the highest mean temperature.
 358 The start day and duration of these events were also significantly correlated with NDVI in
 359 multiple regression, albeit with a weaker R^2 (Fig. 3b; $F = 3.802$, D.F. = 3, 29, $p < 0.05$, $R^2 =$
 360 0.21). In both cases there was a significant interaction between the two model predictors (start
 361 day and mean temperature), meaning that the effect of start day on NDVI was weaker for longer
 362 events.

363

364

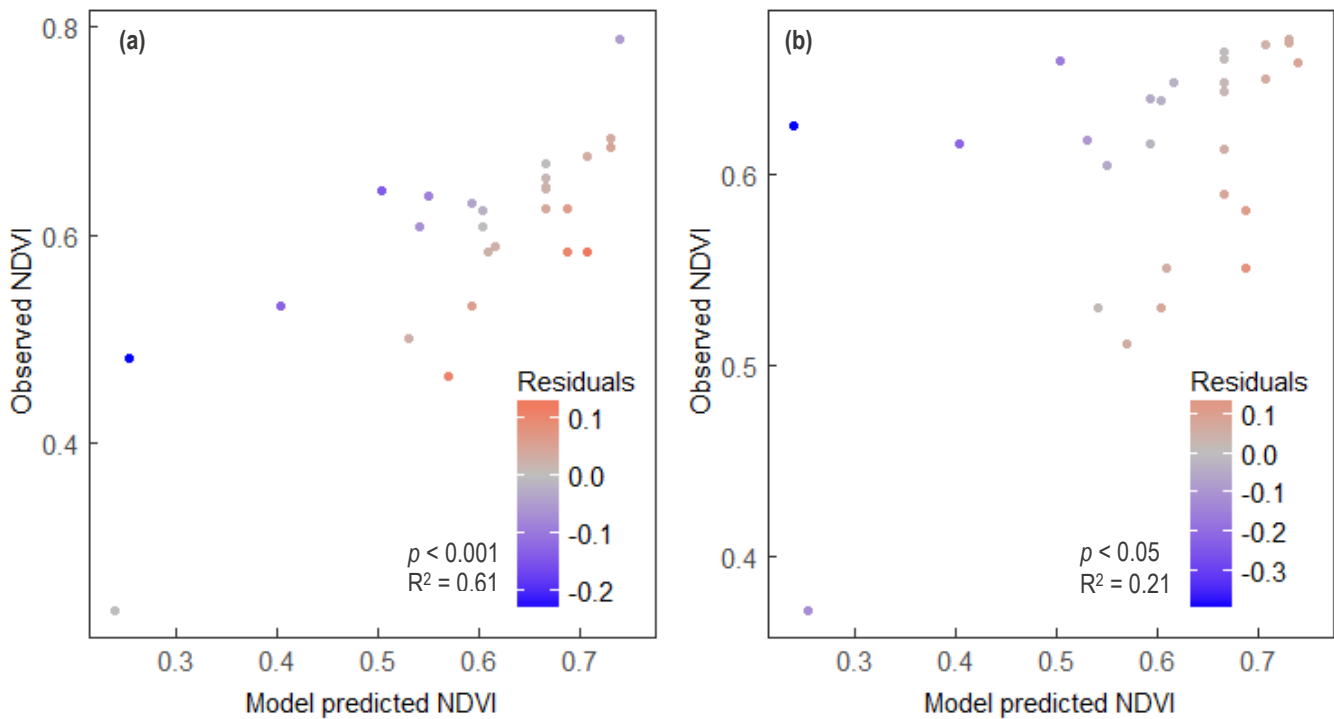


Figure 3: Correlations between plot-level NDVI as predicted by multiple regression models and plot-level NDVI observed in the field. Correlations are shown for (a) ‘Maximum duration exposure events’ and (b) ‘Maximum warmth exposure events’. Points are coloured according to the value of residuals; warm colouring indicates that multiple regression predicted higher NDVI values than were observed in the field, while cold colouring indicates that multiple regression predicted lower NDVI values than observed.

365

366 **3.2 Climate metrics in regional scale analyses**

367

368 Climate metrics calculated and mapped across the Norwegian Arctic implicate the processes
369 underlying frost drought and extreme winter warming in MODIS NDVI change between the
370 2005-2010 baseline period and 2014. They also highlight interesting characteristics of winter
371 climate and the conditions which lead to extreme climatic event-driven browning.

372

373 *3.2.1 Event characteristics*

374 Maximum intensity warming event metrics (intensity, start day and mean snow cover) show
375 that prolonged periods of warmth during winter were rare across the Norwegian Arctic region

376 in the 2013/14 winter (indicated by low maximum intensity across much of the region; Fig 4a).
377 Such rare occurrence is consistent with climatic conditions which can produce an ecologically
378 extreme response (i.e. extreme events). The median value of intensity in the 2013/14 winter
379 was 61 across the entire Norwegian Arctic region, compared to a median of 328 specifically in
380 observed browning sites. The wide variation inherent in this variable (with a range of 3 to 2440)
381 across the Norwegian Arctic region means that when mapped, areas where events of especially
382 high intensity took place – reflecting prolonged, unseasonable warmth – are clearly
383 distinguishable by eye (Fig 4a). Visual assessment suggests that high intensity events, when
384 they do occur, are most often found in coastal areas. Furthermore, while most warming events
385 across the region occurred in the first half of the winter period, with 60% occurring in January
386 alone, events with the highest maximum intensity typically began later in the season (Fig 4;
387 best model: R.S.E = 187.24, D.F = 5265; start day: $t = 9.56$, S.E. = 0.07, $p < 0.001$). There was
388 no significant correlation between event intensity and mean snow cover during the event.

389

390

391

392

393

394

395

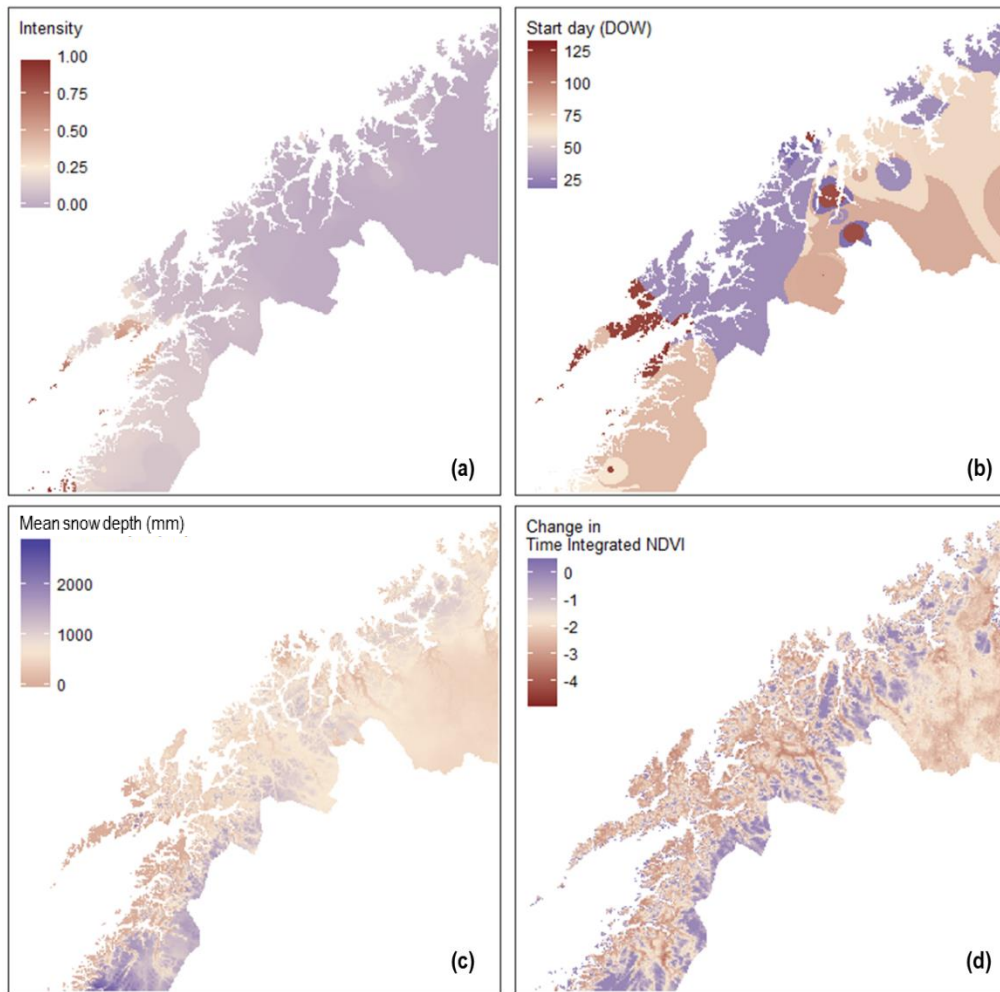


Figure 4: Climate metrics calculated for the warmth event with the highest intensity in each 1 km² pixel. Climate metrics shown are (a) intensity; cumulative warmth weighted linearly by event duration, here rescaled to a range of 0-1 for easier interpretation, (b) the start day of the event (Day of Winter 1 equivalent to Day of Year 305) and (c) mean snow depth (mm) during the event. The change in time integrated NDVI between the baseline 2005-2010 period and 2014 is shown (d) for comparison with the potential climatic drivers (a) – (c).

396

397 Similarly, exposure event metrics show that exposure (snow depth = 0) during winter was
 398 relatively rare across the Norwegian Arctic in the 2013/14 winter (Fig. 5a) and was limited
 399 primarily to coastal areas. Where exposure events did take place further inland, visual
 400 comparison suggests they typically began later in the winter compared to those taking place
 401 close to the coastline (Fig. 5b). All winter 2013/14 exposure events across observed browning
 402 sites plus the majority (59 %) of exposure events across the Norwegian Arctic region were

403 associated with a mean air temperature of more than 0 °C during the event. However, 21 % of
404 Norwegian Arctic-region exposure events were relatively cold, with mean air temperature
405 below or equal to -2 °C. Visual comparison suggests these cold exposure events may be more
406 common further inland. Timing of the longest exposure events across the region was relatively
407 evenly spread throughout the majority of the winter period, although with a higher proportion
408 (32 %) of events occurring in April.

409

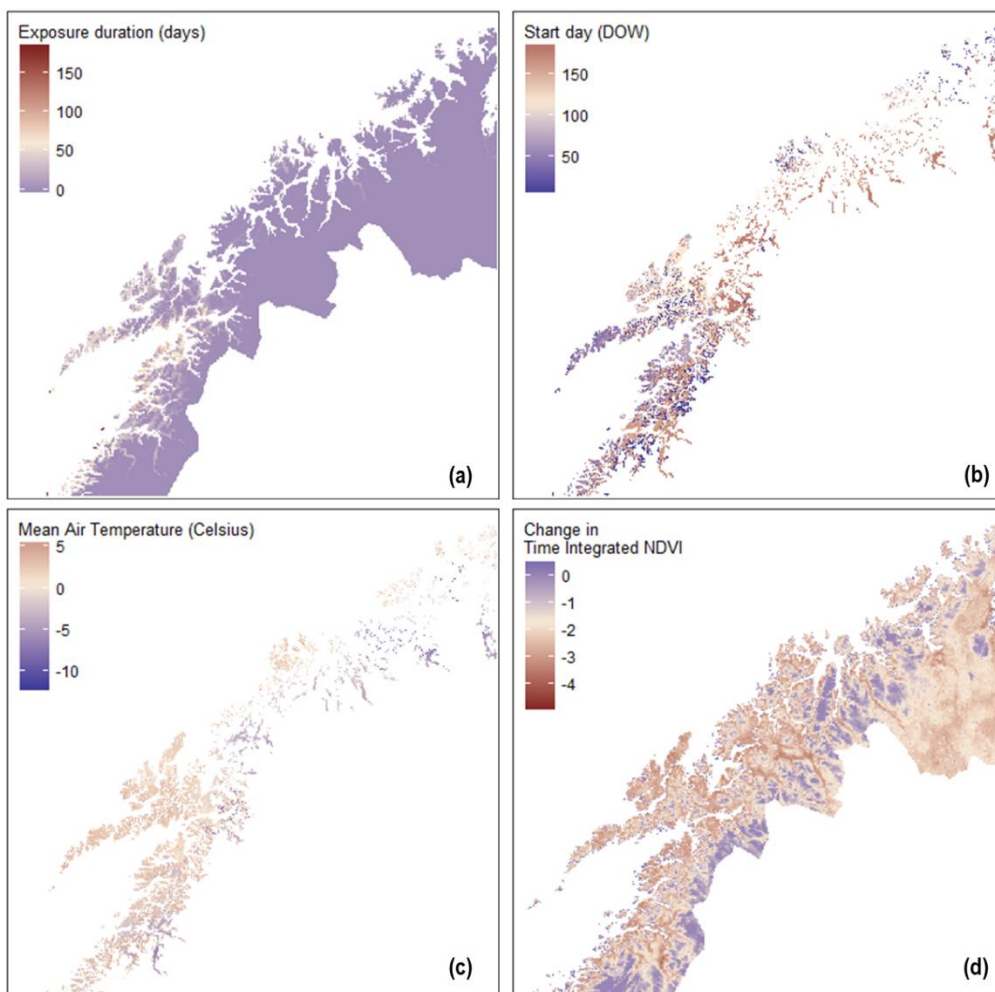


Figure 5: Climate metrics calculated for the exposure event with the longest duration in each 1 km² pixel. Climate metrics shown are (a) event duration (b) the start day of the event (Day of Winter 1 equivalent to Day of Year 305) and (c) mean air temperature (°C) during the event. The change in time integrated NDVI between the baseline 2005-2010 period and 2014 is shown (d) for comparison with the potential climatic drivers (a) – (c).

410

411 3.2.2 *Correlation with MODIS NDVI*

412 *Maximum intensity warm events*: both the intensity of the event (Fig. 4a), and the mean snow
413 cover during the event (Fig. 4c) were significantly positively correlated with change in time
414 integrated NDVI (TI-NDVI), i.e. cooler and shorter warming events with shallower snow
415 resulted in greater negative change in TI-NDVI. (Fig. 4d; best model: R.S.E. = 0.54, D.F. =
416 5259; intensity: $t = 2.1$, S.E. < 0.001, $p < 0.05$; mean snow cover: $t = 13.9$, S.E. < 0.001, $p <$
417 0.001). There was also a significant negative interaction between intensity and mean snow
418 cover ($t = -5.19$, S.E. < 0.001, $p < 0.001$) and, while the start day of the event did not have a
419 significant main effect, there was a significant positive three-way interaction between intensity,
420 mean snow depth and start day (Fig. 6, $t = 2.56$, S.E. < 0.001, $p < 0.05$). Overall, these terms
421 and interactions show that increasing event intensity (greater air temperature * duration) at the
422 shallowest snow depths results in smaller TI-NDVI reductions (Fig. 6, 25 cm line), while at the
423 deepest snow depths increasing event intensity results in greater TI-NDVI reductions (Fig. 6,
424 100 cm line). As winter progresses (moving left to right on Fig. 6), the slope of the relationship
425 between TI-NDVI change and event intensity becomes more positive at any given snow depth;
426 meaning that the threshold of snow depth above which this slope is negative increases.

427

428 There was no correlation between change in peak-season (July) NDVI and any maximum
429 intensity warm event metric.

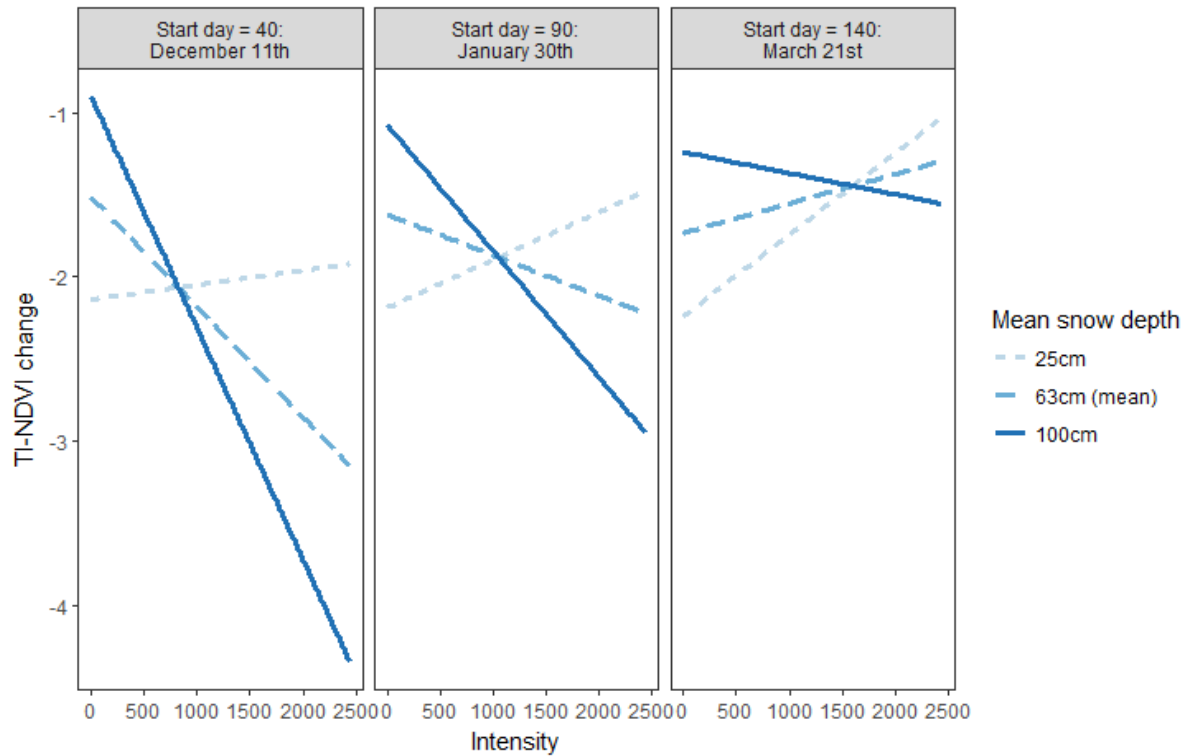


Figure 6: Three-way interaction between intensity (the sum of air temperature multiplied by duration for each day of the event), start day, and mean snow depth in multiple regression of maximum intensity warmth events (the warming event within each pixel with the greatest intensity) with TI-NDVI change. Lines illustrate relationships between event intensity and TI-NDVI change at snow depths of 25cm (short dashed line), the mean value across the Norwegian Arctic Region of 63cm (long dashed line) and 100cm (solid line). Panels show these relationships at different time points during winter.

430

431 *Maximum duration exposure events:* Start day of the longest exposure event (Fig. 5b) was
 432 negatively correlated with change in TI-NDVI, i.e. later longest exposure events resulted in
 433 greater negative NDVI change (best model: R.S.E. = 0.57, D.F. = 2331; start day: $t = -3.91$,
 434 S.E. < 0.001, $p < 0.001$). The mean temperature of the event (Fig. 5c) was positively correlated
 435 with change in TI-NDVI (greater negative TI-NDVI change with cooler events; $t = 3.29$, S.E.
 436 = 0.015, $p < 0.001$), while event duration (Fig. 5a) showed no correlation ($p > 0.05$). There was
 437 an interaction between start day and mean temperature, showing that the slope of the positive

438 relationship between TI-NDVI change and mean temperature became shallower, and
439 eventually became negative, as the winter progressed (Fig. 7 $t = -3.5$, S.E. < 0.001 , $p < 0.001$).

440

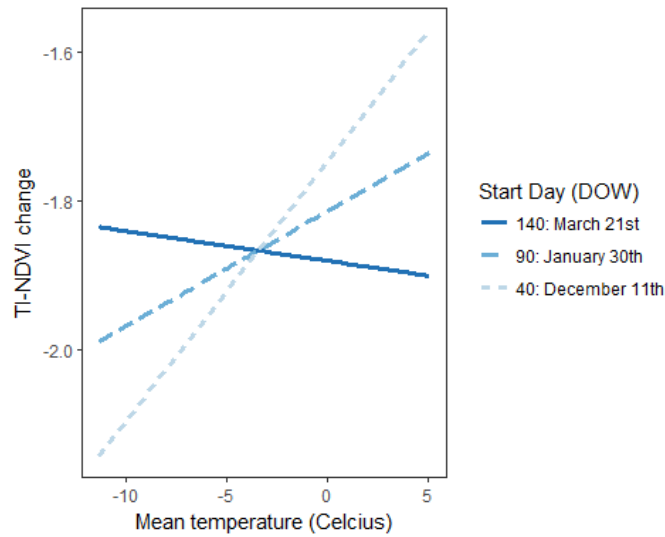


Figure 7: Two-way interaction between the start day and mean air temperature of maximum duration exposure events (periods of consistently absent snow cover with the longest duration in each pixel). Lines illustrate relationships between mean temperature and TI-NDVI change on Day of Winter (DOW) 40 (December 11th; short dashed line), DOW 90 (January 30th; long dashed line) and DOW 140 (March 21st; solid line).

441 There were no correlations between any exposure event metric and change in July NDVI ($p >$
442 0.05).

443

444

445

446

447

448 **4 Discussion**

449

450 We demonstrate that simple climate metrics can explain variation in NDVI (vegetation
451 greenness) in areas known to have been affected by extreme event-driven Arctic browning.

452 These process-based metrics (i) provide quantitative assessment of the climatic conditions that

453 drive browning, reinforcing previous descriptive and qualitative assessments of these climatic

454 drivers by showing that periods of unusual warmth and low snow cover during winter are

455 associated with loss of vegetation greenness (Hancock, 2008; Bjerke et al., 2014, 2017;

456 Bokhorst et al., 2009; Meisingset et al., 2015), and (ii) provide much-needed insight into how

457 variation in these climatic drivers influences the severity of the browning observed. This work

458 also suggests that with further work such metrics, easily calculated from mean daily air

459 temperature and snow depth, could be used to assess the contribution of winter climatic extreme

460 events to Arctic browning at regional scales, and ultimately to improve predictions of how

461 changing Arctic winters will affect the biomass and productivity of vegetation communities.

462

463 **4.1 Plot-level analysis**

464 Metrics representing both maximum intensity warming events (the period of consistently

465 warm, > 2 °C, air temperature with the highest intensity in the plot's pixel, where intensity is

466 the sum of daily mean air temperature multiplied by event duration) and maximum duration

467 exposure events (the period of consistently absent snow cover, 0 mm snow depth, with the

468 longest duration in days in the plot's pixel) explained a substantial proportion of variation in

469 plot-level NDVI across observed browning sites. In analysis of maximum intensity warm

470 events, high intensity, late start date and shallow snow depth were associated with low NDVI.

471 This is consistent with NDVI and biomass reductions driven by extreme winter warming or

472 frost drought events (Bokhorst et al., 2009, Bjerke et al., 2014; Meisingset et al., 2015). In

473 extreme winter warming, unusual winter warmth causes premature dehardening and initiation
474 of spring-like bud-burst following snow melt and exposure of vegetation to warmth, after
475 which the rapid return of sub-zero temperatures causes frost damage (Phoenix & Lee, 2004;
476 Bokhorst et al., 2008). It is likely that vegetation could be more prone to extreme winter
477 warming damage later in winter, after a substantial cold period has already been experienced
478 and when light levels are increasing, meaning any subsequent warm period is more likely to
479 trigger premature de-hardening and bud-burst (Körner, 2016; Parmentier et al., 2018).
480 Alternatively, frost drought occurs when vegetation is exposed and soils are frozen, which
481 reduces the availability of free water and promotes winter desiccation (Tranquillini 1982; Sakai
482 & Larcher, 2012). In late winter, soils are most likely to be closer to their coldest year-round
483 temperature. Exposure events with a higher mean air temperature at this time may therefore
484 encourage plant transpiration and water loss, but may not be sufficiently warm to initiate soil
485 thaw and an increase in the availability of free water (Larcher & Siegwolf, 1987). Desiccation
486 is likely to be further accelerated in late winter due to higher solar irradiance, which promotes
487 physiological activity including transpiration and increasing water loss (Hadley & Smith, 1986,
488 1989). However, since there is a high explanatory power of the 24-h drop in temperature
489 following the end of the warm period, it appears likely that the browning observed at these sites
490 is driven largely by extreme winter warming rather than frost drought.

491

492 In analysis of maximum duration exposure events, a late start day and comparatively warm
493 mean air temperature (1.7°C) was associated with lower plot-level NDVI, with the negative
494 correlation between mean air temperature and NDVI steepening throughout the winter.
495 Similarly to the above, this could either indicate frost drought or extreme winter warming.
496 Regardless, it would appear that periods of warmth associated with snowmelt or shallow snow
497 depth, particularly in late winter, are strong drivers of the NDVI reductions observed at these

498 sites. This is also consistent with observations that reductions in *Vaccinium myrtillus* biomass
499 in the 2014 growing season in coastal Norway were associated primarily with winter warmth
500 (Meisingset et al., 2015). These results represent a first attempt to disentangle these complex
501 climatic variables and physiological responses. Further work is required to build upon and
502 refine this approach and so develop models with higher explanatory power, as well as models
503 applicable to wider or different Arctic regions.

504

505 **4.2 Regional-scale analysis**

506 Climate metrics calculated for both event types – maximum duration exposure events and
507 maximum intensity warming events – show that both prolonged, warm periods during winter
508 and periods of winter exposure are rare across the Norwegian Arctic region; the majority of the
509 region experienced low maximum intensity of warmth events and no periods of exposure
510 during the 2013/14 winter. This is consistent with ecological theory that states that extreme
511 events should be rare enough that organisms are not (or poorly) adapted to them, such that
512 when these events do occur, an extreme ecological response is produced (Smith 2011). As
513 might be expected, the highest magnitudes of both event types occurred primarily along the
514 coastline, where temperatures are warmer and the climate more variable. As both mean
515 temperatures and temperature variability are expected to increase as climate change progresses
516 (AMAP, 2017), this suggests that coastal areas may act as indicators of conditions likely to
517 become more common as colder, inland areas warm, and supports predictions that the
518 magnitude and frequency of these events will increase across Arctic regions as climate change
519 progresses (Vikhamar-Schuler et al., 2016, Graham et al., 2017).

520

521 Climate metrics for both event types correlated with change in TI-NDVI. For maximum
522 duration exposure events the strongest predictor of change in TI-NDVI was mean temperature

523 during the exposure event. However, this relationship changes throughout the winter; the
524 negative correlation between start day and change in NDVI (with later events associated with
525 greater TI-NDVI reductions) is steeper where mean temperature is high. This means that early
526 in the winter, cold exposure events are associated with greater TI-NDVI reductions, but in late
527 winter, from around March, it is warmer events that cause larger TI-NDVI reductions. It is
528 these late winter, relatively warm events which contribute to the largest reductions in TI-NDVI
529 overall. Similarly to the plot-level analysis, this could suggest that in late winter, when
530 vegetation has already experienced cold winter temperatures and light availability is increasing,
531 warm conditions may be more likely to initiate premature dehardening, driving extreme winter
532 warming damage (Bokhorst et al., 2010). However, there is also evidence that the impact of
533 exposure events on change in TI-NDVI may be driven to some extent by frost drought. As
534 described above, mild temperatures and high light levels in late winter could accelerate
535 desiccation by encouraging transpiration and water loss before soils begin to thaw (Parmentier
536 et al., 2018). The contrasting link between TI-NDVI reduction and colder temperatures in early
537 winter suggest greater possibility of frost drought as the driving mechanisms of damage: in
538 early winter when normal air temperatures are higher and soils have had little time to chill, cold
539 exposure events may accelerate or exacerbate soil freezing (Hancock, 2008; Zhao et al., 2017),
540 promoting vegetation desiccation.

541

542 For maximum intensity warmth events the strongest predictor of change in TI-NDVI was mean
543 snow depth during the event. Although, overall, maximum intensity warmth events with
544 shallower snow depths were associated with greater TI-NDVI reductions, the relationship
545 between the severity of these events and change in TI-NDVI was determined by interactions
546 between mean snow depth, start day and the intensity of the event. In early winter, increasing
547 event intensity was associated with greater reductions in TI-NDVI when the mean snow depth

548 during those events was deeper. Also, as winter progresses, the relationship between intensity
549 and TI-NDVI becomes shallower, and by late winter increasing event intensity is associated
550 with greater loss of TI-NDVI only at relatively deep snow depths. Overall, this shows that at
551 low temperatures, shallow snow depth and exposure were consistently associated with greater
552 reductions in TI-NDVI. However, these relationships may also reflect smaller impacts of
553 increasingly severe warm spells in vegetation communities which typically experience shallow
554 snow cover or periods of exposure during winter (for example coastal vegetation communities),
555 compared to those where snow cover is typically deep and persistent (Bokhorst et al., 2016).
556 This would arise where vegetation in areas with normally low snow depth may be more adapted
557 and resilient to fluctuations in winter temperature because they typically are (more likely to be)
558 exposed above the snow (Kudo & Hirao, 2006, Bienau et al., 2014). Increasing warming event
559 intensity in these vegetation communities may therefore have little effect. In contrast, areas
560 with greater snow depth may be much more sensitive to extreme temperature fluctuations and
561 higher rates of water loss associated with exposure since here vegetation is typically covered
562 by deep snow throughout winter, and hence is less well adapted to exposure. Further work
563 should determine whether amount of snowmelt (i.e. initial snow depth – final snow depth)
564 during a warming event may be a more ecologically relevant metric than mean snow depth.

565

566 It is not clear why the relationship between change in TI-NDVI and event intensity is positive
567 in late winter, even at mean snow depth (i.e. less negative TI-NDVI change with greater
568 intensity). This may be related to the alleviation of water stress from snow melt-water, or to
569 the impact of increased soil moisture following snowmelt on phenology (Vaganov et al., 1999;
570 Barichivich et al., 2014). Alternatively, it may suggest that late in the winter, when mean air
571 temperatures are beginning to increase, warming events are less likely to be followed by the
572 rapid drop in temperature which was highlighted by plot-level analysis as an important driver

573 of NDVI decline. Without this temperature drop, warming in later winter may simply
574 encourage earlier spring snowmelt and accelerate phenology, without damaging effects
575 (Meisingset et al., 2015). However, this appears to conflict with the association between large
576 NDVI reductions and warm exposure events during late winter, but the reason for these
577 apparently conflicting associations is not clear.

578

579 The regional-scale findings arise from analyses of change in TI-NDVI, yet regional-scale
580 climate metrics did not correlate with change in July NDVI (approximately peak biomass, or
581 peak NDVI). The peak season value of NDVI reflects the seasonal trajectory of photosynthetic
582 activity and can therefore help with interpretation of TI-NDVI (Park et al., 2016). However, it
583 is likely that the influence of altitudinal, latitudinal and coast-inland variability on the timing
584 of peak NDVI, combined with detection of this from just two MODIS images within a single
585 month, means that the genuine peak NDVI may not be well reflected in the methods used here.
586 TI-NDVI may make for better comparison of greenness among sites that have contrasting
587 phenology and timing of peak biomass. In addition, while winter extreme climatic events can
588 drive extensive vegetation mortality, and therefore biomass loss, they also frequently cause
589 severe stress and delayed phenology (Bjerke et al., 2017). Subsequent recovery from stress and
590 catch-up in phenology and/or growth (Koller, 2011; Treharne et al., 2018), would reduce
591 detection from peak season NDVI (Anderson et al., 2016), while the initial stress and
592 phenology impacts would be incorporated in (and likely detected in) TI-NDVI, which
593 correlates with total growing season productivity (Epstein et al., 2017).

594

595 **4.3 Plot-level compared with regional analyses**

596 Analyses at plot-level and regional scales, combined with correlation between plot-level and
597 remotely sensed NDVI (supporting information), indicated similar processes underlying the

598 greatest reductions in NDVI, in particular periods of unusual warmth and exposure during
599 winter, and especially during late winter. However, regional-scale analysis showed more
600 complexity compared to plot-level analysis; for example with colder temperatures during
601 exposure periods associated with greater TI-NDVI reductions in early winter. This illustrates
602 that, while the plot-level analysis focussed on the drivers of pre- and post-damage NDVI in
603 observed browning sites, when these drivers are scaled up to regional analysis, a wider range
604 of processes are involved in NDVI change. As TI-NDVI reflects cumulative productivity
605 across the May – August growing season, reductions in this indicator could reflect altered
606 phenology, and lower productivity in otherwise ‘undamaged’ vegetation, as well as the more
607 extreme ecological responses associated with extreme event-driven browning, such as
608 mortality and visible stress responses (Treharne et al., 2018). Assessing this greater range of
609 conditions driving TI-NDVI change is necessary to investigate the drivers of reductions in
610 greenness observed at landscape to pan-Arctic scales in recent years (Epstein et al., 2015, 2016;
611 Phoenix & Bjerke, 2016; Park et al., 2016). Nonetheless, this work shows that a small number
612 of climate metrics can explain a substantial proportion of variation in NDVI across a region
613 affected by browning in the 2014 growing season. While further work will be required to apply
614 these or similar metrics at a broader scale this demonstrates potential for such simplified
615 approaches requiring a limited range of climate datasets to attribute drivers of browning and
616 be used in models to predict browning in the future.

617

618 **5 Conclusion**

619 This analysis has demonstrated that the severity of NDVI reductions, both across sites where
620 browning has been observed and at a regional scale, can be related to simple, process-based
621 climate metrics. These metrics reinforce ecological theory about the drivers underlying winter
622 climatic extreme event-driven browning, showing that prolonged periods of unusual warmth

623 and vegetation exposure during winter have negative consequences for NDVI. They also
624 provide novel and much-needed insight into how different climatological variables and timing
625 interact to produce greater or less severe browning. Looking forward, with further development
626 utilizing satellite data with medium to high spatial resolution, simple climate metrics could be
627 used to assess the impact of winter extreme climatic event driven-browning on productivity at
628 regional scales and improve predictions of changes in browning frequency in the future.

629

630 **Acknowledgements**

631 RT was supported by the Adapting to the Challenges of a Changing Environment (ACCE)
632 doctoral training partnership, funded by the Natural Environment Research Council (grant
633 award NE/L002450/1). JWB and HT received financial support from the Polish-Norwegian
634 Programme of the EEA Norway Grants (project 198571) and by FRAM–High North Research
635 Centre for Climate and the Environment through its terrestrial flagship program (project
636 362222).

637

638 **Co-author contributions**

639 Project conceived and designed by RT, GKP, JWB and HT.

640 Field data collected by RT, JWB and HT. Data analysis carried out by RT with support from
641 all co-authors.

642 Manuscript preparation led by RT, with support (substantial critical feedback, revisions and
643 additions to text) from all co-authors.

644 Final version of the manuscript read and approved by all co-authors.

645

646 **Highlights**

- 647 • New metrics quantified climatic drivers of extreme event-driven Arctic browning.
- 648 • These metrics explained up to 63% of variation in greenness at affected sites.
- 649 • Prolonged warmth or vegetation exposure in winter are associated with browning.
- 650 • Event metrics correlated with satellite greenness across Arctic Norway.

651

652 **References**

- 653 AMAP, 2017. Snow, Water, Ice and Permafrost in the Arctic (SWIPA) 2017. Arctic
654 Monitoring and Assessment Programme (AMAP), Oslo, Norway. xiv + 269.
- 655 Anderson, H. B., Nilsen, L., Tømmervik, H., Karlsen, S. R., Nagai, S. & Cooper, E. J., 2016.
656 Using ordinary digital cameras in place of near-infrared sensors to derive vegetation indices
657 for phenology studies of High Arctic vegetation. *Remote Sensing*, 8, 847,
658 doi:10.3390/rs8100847.
- 659 Altwegg, R., Visser, V., Bailey, L. D., & Erni, B., 2017. Learning from single extreme events.
660 *Phil. Trans. R. Soc. B*, 372, 20160141. <https://doi.org/10.1098/rstb.2016.0141>
- 661 Bailey, L. D., & van de Pol, M., 2016. Tackling extremes: challenges for ecological and
662 evolutionary research on extreme climatic events. *Journal of Animal Ecology*, 85, 85–96.
663 <https://doi.org/10.1111/1365-2656.12451>
- 664 Bjerke J. W., Karlsen S. R., Høgda K. A. et al., 2014. Record-low primary productivity and
665 high plant damage in the Nordic Arctic Region in 2012 caused by multiple weather events and
666 pest outbreaks. *Environmental Research Letters*, 9, 084006. [https://doi.org/10.1088/1748-](https://doi.org/10.1088/1748-9326/9/8/084006)
667 [9326/9/8/084006](https://doi.org/10.1088/1748-9326/9/8/084006).
- 668 Bjerke J. W., Treharne R., Vikhamar-Schuler D. et al., 2017. Understanding the drivers of
669 extensive plant damage in boreal and Arctic ecosystems: Insights from field surveys in the
670 aftermath of damage. *Science of The Total Environment*, 599–600, 1965–1976.
671 <https://doi.org/10.1016/j.scitotenv.2017.05.050>.
- 672 Bokhorst S., Bjerke J. W., Bowles F. W., Melillo J., Callaghan T. V., & Phoenix G. K., (2008).
673 Impacts of extreme winter warming in the sub-Arctic: growing season responses of dwarf shrub
674 heathland. *Global Change Biology*, 14, 2603–2612. [https://doi.org/10.1111/j.1365-](https://doi.org/10.1111/j.1365-2486.2008.01689.x)
675 [2486.2008.01689.x](https://doi.org/10.1111/j.1365-2486.2008.01689.x)
- 676 Bokhorst, S., Bjerke, J. W., Street, L. E., Callaghan, T. V., & Phoenix, G. K., 2011. Impacts of
677 multiple extreme winter warming events on sub-Arctic heathland: phenology, reproduction,
678 growth, and CO₂ flux responses. *Global Change Biology*. 17, 2817–2830.
679 <https://doi.org/10.1111/j.1365-2486.2011.02424.x>
- 680 Bokhorst, S. F., Bjerke, J. W., Tømmervik, H., Callaghan, T. V., & Phoenix, G. K., 2009.
681 Winter warming events damage sub-Arctic vegetation: consistent evidence from an

682 experimental manipulation and a natural event. *Journal of Ecology*, 97, 1408–1415.
683 <https://doi.org/10.1111/j.1365-2745.2009.01554.x>

684 Bourgeon, M. A., Gee, C., Debuissou, S., Villette, S., Jones, G., & Paloli, J. N., 2017. « On-
685 the-go » multispectral imaging system to characterize the development of vineyard foliage with
686 quantitative and qualitative vegetation indices. *Precision Agriculture*, 18, 293–308.

687 Burnham, K. P., & Anderson, D. R. (2002). *Model Selection and Multimodel Inference: A*
688 *Practical Information-Theoretic Approach*. Springer Science & Business Media, New York.

689 Denny, M. W., Hunt, L. J. H., Miller, L. P., & Harley, C. D. G., 2009. On the prediction of
690 extreme ecological events. *Ecological Monographs*, 79, 397–421. [https://doi.org/10.1890/08-](https://doi.org/10.1890/08-0579.1)
691 [0579.1](https://doi.org/10.1890/08-0579.1)

692 Easterling, D. R., Meehl, G. A., Parmesan, C., Changnon, S. A., Karl, T. R., & Mearns, L. O.,
693 2000. Climate extremes: observations, modelling, and impacts. *Science*, 289, 2068–2074.
694 <https://doi.org/10.1126/science.289.5487.2068>

695 Epstein H. E., Bhatt U.S., Raynolds M. K., et al. (2015) Tundra Greenness. In: Arctic Report
696 Card: Update for 2015 (eds Jeffries MO, Richter-Menge J., Overland J. E.). NOAA, Silver
697 Spring, MD. Available at: <http://www.arctic.noaa.gov/reportcard/>

698 Epstein H. E., Bhatt U.S., Raynolds M. K., et al. (2016) Tundra Greenness. In: Arctic Report
699 Card: Update for 2016 (eds Richter-Menge J., Overland J. E., Mathis, J. T.). NOAA, Silver
700 Spring, MD. Available at: <http://www.arctic.noaa.gov/reportcard/>

701 Graham, R. M., Cohen, L., Petty, A. A. et al., 2017. Increasing frequency and duration of Arctic
702 winter warming events. *Geophysical Research Letters*, 44, 6974–6983.
703 <https://doi.org/10.1002/2017GL073395>

704 Gutschick, V. P., & BassiriRad, H., 2003. Extreme events as shaping physiology, ecology, and
705 evolution of plants: toward a unified definition and evaluation of their consequences. *New*
706 *Phytologist*, 160, 21–42. <https://doi.org/10.1046/j.1469-8137.2003.00866.x>

707 Hadley, J. L., & Smith, W. K., 1989. Wind erosion of leaf surface wax in alpine timberline
708 conifers. *Arctic and Alpine Research*, 21, 392–398. <https://doi.org/10.2307/1551648>

709 Hadley, J. L., & Smith, W. K., 1986. Wind effects on needles of timberline conifers: seasonal
710 influence on mortality. *Ecology*, 67, 12–19. <https://doi.org/10.2307/1938498>

711 Hancock, M. H., 2008. An exceptional *Calluna vulgaris* winter die-back event, Abernethy
712 Forest, Scottish Highlands. *Plant Ecology & Diversity*, 1, 89–103.
713 <https://doi.org/10.1080/17550870802260772>

714 Hoover, D. L., & Rogers, B. M., 2016. Not all droughts are created equal: the impacts of
715 interannual drought pattern and magnitude on grassland carbon cycling. *Global Change*
716 *Biology*, 22, 1809–1820. <https://doi.org/10.1111/gcb.13161>

717 Hørbye J. 1882. Om frostskaeder paa barskoven [On frost damage to the conifer forests]. *Den*
718 *Norske Forstforenings Aarbog*, 99-105.

719 Horton, R. M., Mankin, J. S., Lesk, C., Coffel, E., & Raymond, C., 2016. A review of recent
720 advances in research on extreme heat events. *Current Climate Change Reports*, 2, 242–259.
721 <https://doi.org/10.1007/s40641-016-0042-x>

722 Jentsch, A., Kreyling, J., & Beierkuhnlein, C., 2007. A new generation of climate-change
723 experiments: events, not trends. *Frontiers in Ecology and the Environment*, 5, 365–374.
724 [https://doi.org/10.1890/1540-9295\(2007\)5\[365:ANGOCE\]2.0.CO;2](https://doi.org/10.1890/1540-9295(2007)5[365:ANGOCE]2.0.CO;2)

725 Jepsen, J. U., Biuw, M., Ims, R. A., Kapari, L., Schott, T., Vindstad, O. P. L., & Hagen, S. B.,
726 2013. Ecosystem impacts of a range expanding forest defoliator at the forest-tundra ecotone.
727 *Ecosystems*, 16, 561–575. <https://doi.org/10.1007/s10021-012-9629-9>

728 Knapp, A. K., Hoover, D. L., Wilcox, K. R. et al., 2015. Characterizing differences in
729 precipitation regimes of extreme wet and dry years: implications for climate change
730 experiments. *Global Change Biology*, 21, 2624–2633. <https://doi.org/10.1111/gcb.12888>

731 Koller, E. K., 2011. Controls on the growth of three subarctic dwarf shrubs along the
732 Kårsavagge catchment gradient. Chapter 2 in: *Impacts of environmental change on subarctic*
733 *dwarf shrub communities: landscape gradient and field manipulation approaches*. PhD thesis,
734 University of Sheffield.

735 Kudo, G., & Hirao, A. S., 2006. Habitat-specific responses in the flowering phenology and
736 seed set of alpine plants to climate variation: implications for global-change impacts.
737 *Population Ecology*, 48, 49–58. <https://doi.org/10.1007/s10144-005-0242-z>

738 Larcher, W., & Siegwolf, R., 1985. Development of acute frost drought in *Rhododendron*
739 *ferrugineum* at the alpine timberline. *Oecologia*, 67, 298–300.
740 <https://doi.org/10.1007/BF00384304>

741 Lloyd-Hughes, B., 2012. A spatio-temporal structure-based approach to drought
742 characterisation. *International Journal of Climatology*, 32, 406–418.
743 <https://doi.org/10.1002/joc.2280>

744 Mahecha, M. D., Gans, F., Sippel, S., et al., 2017. Detecting impacts of extreme events with
745 ecological in situ monitoring networks. *Biogeosciences*, 14, 4255–4277.
746 <https://doi.org/10.3929/ethz-b-000192472>

747 Meisingset, E. L., Austrheim, G., Solberg, E., Brekkum, Ø., & Lande, U. S., 2015. Effekter av
748 klimastress på hjortens vinterbeiter [Effects of climatic stress on red deer browsing –
749 development of bilberry after an extreme weather event during the winter of 2014]. Utvikling
750 av blåbærlyngen etter tørkevinteren 2014, NIBIO Rapport, 1 (64), 28 pp.
751 <http://hdl.handle.net/11250/2368503>

752 Niu, S., Luo, Y., Li, D., Cao, S., Xia, J., Li, J., & Smith, M. D., 2014. Plant growth and mortality
753 under climatic extremes: An overview. *Environmental and Experimental Botany*, 98, 13–19.
754 <https://doi.org/10.1016/j.envexpbot.2013.10.004>

755 Park, T., Ganguly, S., Tømmervik, H., Euskirchen, E.S., Høgda, K.A., Karlsen, S.R., Brovkin,
756 V., Nemani, R.R., & Myneni, R. B., 2016. Changes in growing season duration and
757 productivity of northern vegetation inferred from long-term remote sensing data.
758 *Environmental Research Letters*, 11, 084001. doi:10.1088/1748-9326/11/8/084001.

759 Parmentier, F.-J. W., Rasse, D. P., Lund, M., et al., 2018. Vulnerability and resilience of the
760 carbon exchange of a subarctic peatland to an extreme winter event. *Environmental Research*
761 *Letters*, 13, 065009. <https://doi.org/10.1088/1748-9326/aabff3>

762 Parmesan, C., 2006. Ecological and evolutionary responses to recent climate change. *Annual*
763 *Review of Ecology, Evolution, and Systematics*, 37, 637–669.
764 <https://doi.org/10.1146/annurev.ecolsys.37.091305.110100>

765 Pettorelli, N., Vik, J. O., Myrsterud, A., Gaillard, J.-M., Tucker, C. J., & Stenseth, N. C., 2005.
766 Using the satellite-derived NDVI to assess ecological responses to environmental change.
767 *Trends in Ecology & Evolution*, 20, 503–510. <https://doi.org/10.1016/j.tree.2005.05.011>

768 Phoenix, G. K., & Bjerke, J. W., 2016. Arctic browning: extreme events and trends reversing
769 arctic greening. *Global Change Biology*, 22, 2960–2962. <https://doi.org/10.1111/gcb.13261>

770 Phoenix, G. K., & Lee, J. A., 2004. Predicting impacts of Arctic climate change: past lessons
771 and future challenges. *Ecological Research*, 19, 65–74. <https://doi.org/10.1111/j.1440->
772 1703.2003.00609.x

773 Post, E., Forchhammer, M. C., Bret-Harte, M. S. et al., 2009. Ecological dynamics across the
774 Arctic associated with recent climate change. *Science*, 325, 1355–1358.
775 <https://doi.org/10.1126/science.1173113>

776 Printz, H. 1933. Granens og furuens fysiologi og geografiske utbredelse [The physiology and
777 geographical distribution of Norway spruce and Scots pine]. *Nyt Magazin for*
778 *Naturvidenskaberne B.* 73: 167-219.

779 Reichstein, M., Bahn, M., Ciais, P. et al., 2013. Climate extremes and the carbon cycle. *Nature*,
780 500, 287–295. <https://doi.org/10.1038/nature12350>

781 Rouse, J.W., Hass, R.H., Schell, J.A., & Deering, D.W., 1973. Monitoring vegetation systems
782 in the great plains with ERTS. In Proc. 3rd Earth Resources Technology Satellite (ERTS)
783 Symposium, Washington, DC, USA: NASA SP-351, NASA, Vol 1, 309–17.

784 Sakai, A., & Larcher, W., 2012. *Frost Survival of Plants: Responses and Adaptation to Freezing*
785 *Stress*. Springer Science & Business Media.

786 Sarojini, B. B., Stott, P. A., & Black, E., 2016. Detection and attribution of human influence
787 on regional precipitation. *Nature Climate Change*, 6, 669–675.
788 <https://doi.org/10.1038/nclimate2976>

789 Sillmann, J., & Roeckner, E., 2008. Indices for extreme events in projections of anthropogenic
790 climate change. *Climatic Change*, 86, 83–104. <https://doi.org/10.1007/s10584-007-9308-6>

791 Sippel, S., Zscheischler, J., & Reichstein, M., 2016. Ecosystem impacts of climate extremes
792 crucially depend on the timing. *Proceedings of the National Academy of Sciences*, 113, 5768–
793 5770. <https://doi.org/10.1073/pnas.1605667113>

794 Smith, M. D., 2011. An ecological perspective on extreme climatic events: a synthetic
795 definition and framework to guide future research: Defining extreme climate events. *Journal*
796 *of Ecology*, 99, 656–663. <https://doi.org/10.1111/j.1365-2745.2011.01798.x>

797 Solow, A. R., 2017. On detecting ecological impacts of extreme climate events and why it
798 matters. *Phil. Trans. R. Soc. B*, 372, 20160136. <https://doi.org/10.1098/rstb.2016.0136>

799 Stow, D. A., Hope, A., McGuire, D. et al., 2004. Remote sensing of vegetation and land-cover
800 change in Arctic tundra ecosystems. *Remote Sensing of Environment*, 89, 281-308.
801 <https://doi.org/10.1016/j.rse.2003.10.018>

802 Treharne, R., Bjerke, J. W., Tømmervik, H., Stendardi, L., & Phoenix, G. K. Arctic browning:
803 Impacts of extreme climatic events on heathland ecosystem CO₂ fluxes. *Global Change*
804 *Biology*, in press. <https://doi.org/10.1111/gcb.14500>

805 Ummenhofer, C. C., & Meehl, G. A., 2017. Extreme weather and climate events with
806 ecological relevance: a review. *Phil. Trans. R. Soc. B*, 372, 20160135.
807 <https://doi.org/10.1098/rstb.2016.0135>.

808 Van de Pol, M., Jenouvrier, S., Cornelissen, J. H. C., & Visser, M. E., 2017. Behavioural,
809 ecological and evolutionary responses to extreme climatic events: challenges and directions.
810 *Phil. Trans. R. Soc. B*, 372, 20160134. <https://doi.org/10.1098/rstb.2016.0134>

811 Vasseur, D. A., DeLong, J. P., Gilbert, B. et al., 2014. Increased temperature variation poses a
812 greater risk to species than climate warming. *Proceedings of the Royal Society of London B:*
813 *Biological Sciences*, 281, 20132612. <https://doi.org/10.1098/rspb.2013.2612>

814 Vikhamar-Schuler, D., Isaksen, K., Haugen, J. E., Tømmervik, H., Luks, B., Schuler, T. V., &
815 Bjerke, J. W., 2016. Changes in winter warming events in the Nordic Arctic Region. *Journal*
816 *of Climate*, 29, 6223–6244. <https://doi.org/10.1175/JCLI-D-15-0763.1>

817 Williams, C. M., Henry, H. A. L., & Sinclair, B. J. (2015). Cold truths: how winter drives
818 responses of terrestrial organisms to climate change. *Biological Reviews*, 90, 214–235.
819 <https://doi.org/10.1111/brv.12105>

820 Wolf, S., Keenan, T. F., Fisher, J. B. et al., 2016. Warm spring reduced carbon cycle impact of
821 the 2012 US summer drought. *Proceedings of the National Academy of Sciences*, 113, 5880–
822 5885. <https://doi.org/10.1073/pnas.1519620113>

823 Zeppel, M. J. B., Wilks, J. V., & Lewis, J. D., 2014. Impacts of extreme precipitation and
824 seasonal changes in precipitation on plants. *Biogeosciences; Katlenburg-Lindau*, 11, 3083.
825 <https://doi.org/http://dx.doi.org/10.5194/bg-11-3083-2014>

826 Zscheischler, J., Mahecha, M. D., von Buttlar, J. et al., 2014. A few extreme events dominate
827 global interannual variability in gross primary production. *Environmental Research Letters*, 9,
828 035001. <https://doi.org/10.1088/1748-9326/9/3/035001>

829 Zscheischler, J., Mahecha, M. D., Harmeling, S., & Reichstein, M., 2013. Detection and
830 attribution of large spatiotemporal extreme events in Earth observation data. *Ecological*
831 *Informatics*, 15, 66–73. <https://doi.org/10.1016/j.ecoinf.2013.03.004>